

Theoretical Investigation on the Dispersion of Graded-Index Polymer Optical Fibers

Gnitabouré Yabre, *Member, IEEE*

Abstract—Various experiments on polymer optical fibers (POF's) suggest that they present a large transmission capacity, but this is not confirmed by the standard theory. In this paper we present a full dispersion model based on evaluating the frequency response of the fiber instead of the direct calculation of the pulse broadening from the moments of the impulse response. The mathematical formalism is firstly displayed and subsequently applied to the graded-index POF made with polymethylmethacrylate (PMMA). The simulation results show that the baseband bandwidth is indeed enhanced due to the strong differential mode attenuation (DMA).

Index Terms—Bandwidth, differential mode attenuation, dispersion, optical communications, polymer optical fibers.

I. INTRODUCTION

POLYMER optical fibers (POF's) are being developed as important high-speed communication media for short- and medium-distance applications. Polymer fibers including the step-index as well as the graded-index versions have a large core-diameter (500–1500 μm) and a large numerical aperture (0.2–0.9), which allows for easy connectorization of systems and efficient launching from semiconductor lasers or light emitting diodes. Furthermore, they show a complete immunity to EMI/EMR (electromagnetic interference/electromagnetic radiation) and a great resistance to mechanical damage as a consequence of the intrinsic flexibility of the polymer material. On the other hand, the graded-index type polymer optical fiber (GIPOF) can combine these properties with a large capacity for digital transmission. Accordingly, the GIPOF as a physical transmission medium is foreseen to be the best candidate for the replacement of the metallic cables traditionally used in customer premises networks (CPN's), interconnect and access links. The utilization of conventional glass optical fibers (GOF's) could also be envisaged in these applications, but the corresponding connectors are expensive. In addition, the fabrication and termination of GOF's are more difficult than those of POF's and also the glass material is more expensive than polymer, so the cost of the overall GOF-based system would be inevitably high.

A number of researchers has previously demonstrated that undistorted bit streams of 2.5 Gb/s could be transmitted through the polymethylmethacrylate (PMMA) GIPOF over a distance

of 100 m [1], [2]. In more recent experiments [3], [4], we successfully reached the record transmission length of 200 m. A full description of the state of the art regarding POF's and related technologies is to appear in [5]. However, the achievements have been accomplished so far without real reference to prediction tools. The existing simulation models have been developed for GOF systems some decades ago and involve some approximations that appear invalid in consideration of polymer optical fibers. On the basis of the standard theory as it will be clarified further, the error-free transmission experiment at 2.5 Gb/s over a 200-m-long fiber that we successfully carried out in [3], [4] would have been rather problematic.

In the present work, we solve the above discrepancy and show that the factors that have until now been given little attention can have a large impact on the data rate transmission performance. This model presents a full description of the dispersion which incorporates all the parameters involved in the determination of the total bandwidth. It is based on analytically evaluating the frequency response of the fiber instead of the direct calculation of the pulse broadening from the moments of the impulse response. We show that the baseband bandwidth is indeed increased in GIPOF's mainly due to the strong differential mode attenuation (DMA). Actually, this illustrates the classical conflicting relation between dispersion and loss in multimode fibers (MMF's) in general. As a matter of fact, the large DMA of high-order modes necessarily causes a large power penalty during light propagation, but at the same time it yields a bandwidth enhancement as a result of the mode stripping effect.

To make it easy to apply the present analysis to any multimode optical fiber link, the mathematical formalism is explicitly displayed before specific computer simulations applied to the PMMA-type GIPOF doped with benzyl benzoate (BEN) are presented and discussed through illustrative curves. We achieved a more than fourfold enhancement in the baseband bandwidth in the presence of DMA even if a complete mode filling condition is imposed at the input end of the fiber.

II. THEORY

We consider the class of circular-symmetric fibers described by the refractive index profile

$$n(r, \lambda) = \begin{cases} n_1(\lambda)[1 - 2\Delta(\lambda)(r/a)^\alpha]^{1/2} & \text{for } 0 \leq r \leq a \\ n_1(\lambda)[1 - 2\Delta(\lambda)]^{1/2} & \text{for } r \geq a \end{cases} \quad (1)$$

where r is an offset distance from the core center, α is the core index exponent ($\alpha > 0$), λ is the free-space wavelength, $n_1(\lambda)$ is the refractive index in the center of the core, $\Delta(\lambda)$ is the refractive-index contrast, a is the core radius (i.e., the

Manuscript received August 17, 2000; revised February 16, 2000. This work was supported and conducted within the framework of the Dutch research project IOP Electro-Optics ongoing in the COBRA research institute, Eindhoven University of Technology.

The author is with COBRA, Interuniversity Research Institute, Eindhoven University of Technology, EH 12.33, Eindhoven 5600 MB, The Netherlands.

Publisher Item Identifier S 0733-8724(00)05077-5.

radius at which the index $n(r, \lambda)$ reaches the cladding value $n_2(\lambda) = n_1(\lambda)[1 - 2\Delta(\lambda)]^{1/2}$. For the following, we will simply use the identifications $n_1 = n_1(\lambda)$, $n_2 = n_2(\lambda)$ and $\Delta = \Delta(\lambda)$, and let the quantities dependence on wavelength be implicit.

Multimode optical fibers described by (1) potentially support a large but finite number of modes which are particular solutions of the Maxwell's equations. Each guided mode has its own propagation constant and therefore propagates at its own particular velocity. From the WKB analysis it was shown that propagated modes are actually clustered within groups in which each mode has nearly the same propagation constant derived to be [6]

$$\beta = 2\pi \frac{n_1}{\lambda} \left[1 - 2\Delta \left(\frac{m}{M} \right)^{2\alpha/(\alpha+2)} \right]^{1/2} \quad (2)$$

where m is the principal mode group number (or principal mode group order) and M is the total number of mode groups that can potentially be excited. M is analytically given by

$$M = 2\pi a \frac{n_1}{\lambda} \left(\frac{\alpha\Delta}{\alpha+2} \right)^{1/2} \quad (3)$$

The modal delay per unit length can be derived from (2) using the definition $\tau(x) = -\lambda^2 \beta' / (2\pi c)$ where the prime denotes the derivation with respect to wavelength and c is the speed of light in vacuum. The calculation leads to

$$\tau(x) = \frac{N_1}{c} \left[1 - \frac{\Delta(4+\epsilon)}{\alpha+2} x^{2\alpha/(\alpha+2)} \right] \cdot \left[1 - 2\Delta x^{2\alpha/(\alpha+2)} \right]^{-1/2} \quad (4)$$

in which N_1 is the group index and ϵ is the profile dispersion parameter, respectively, given by

$$N_1 = n_1 - \lambda n_1' \quad (5)$$

$$\epsilon = \frac{-2n_1}{N_1} \frac{\lambda \Delta'}{\Delta}. \quad (6)$$

For further use, let us also express the difference in propagation constant between adjacent mode groups. Considering level m and level $m+1$, the spacing is approximately given by $\delta\beta \simeq \partial\beta/\partial m$, which yields

$$\delta\beta = -\frac{2}{a} \left(\frac{\alpha\Delta}{\alpha+2} \right)^{1/2} \left(\frac{m}{M} \right)^{(\alpha-2)/(\alpha+2)}. \quad (7)$$

A. Background

So far two different analytic approaches have been used to evaluate the pulse dispersion in polymer optical fibers [7], [8]. The approach taken in [7] is based on Olshansky and Keck's theory [6] which assumes a uniform excitation and neglects both distributed loss and mode-coupling. Moreover, these parameters, in particular the distributed loss, may have a significant impact as we show further.

The approach taken in [8] is an attempt to incorporate the mode-coupling effect in the dispersion model by using the following bandwidth formula derived in [9]:

$$BW = BW_0 \left(\frac{z}{z_c} \right)^{1/2} \quad (8)$$

where z is the transmission distance and z_c is the so-called coupling length, BW_0 being the corresponding bandwidth. But this model uses the uniform launching assumption and also ignores the DMA [9]. Furthermore, it no longer associates the contribution of the material dispersion which is known to be strong in POF's. On the other hand, the right hand side of formula (8) contains two unknowns, that is, BW_0 and z_c that are dependent on the launching conditions and therefore difficult to put on accurate numerical values. Any attempt to measure BW_0 and z_c should be altered by a large error because the effect of DMA and that of chromatic dispersion cannot be prevented from affecting the results. The coupling length was estimated in [8] to be 2 m, but this value seems too small for ordinary GIPOF's. This view is supported by the fact that the suggested coupling-length of 2 m is not confirmed by measurements. In the reality, the effect of mode-coupling in GIPOF should be negligible for the following reason. The length-dependent mode-coupling is a diffusion process resulting from small power exchanges on imperfections along the fiber. These exchanges can cause the modal delay times to be averaged [10] and consequently a bandwidth enhancement if the transmission distance is long enough for each propagated mode to undergo a statistically large number of interactions before detection. This requirement appears to be unsatisfied if the transmission length is limited to a few hundred meters as it is for instant the case. This explanation can be best understood by reference to numerical values which compare the graded-index POF with a graded-index GOF.

Propagated modes belonging to different groups most easily interchange energy when they have field distribution that strongly overlap, and fiber imperfections are most effective in causing this when they present a periodicity equal to the beat period of the two modes in consideration. If this criterion is fulfilled, the coupling between level m and level $m+1$ adds in phase from one interaction to the next and becomes considerable. In other words, if we assume that the perturbations are periodic with "wavelength" Λ , the mode-mixing is strongest when $\Lambda = 2\pi/|\delta\beta|$ [with $\delta\beta$ being given by (7)]. For a parabolic standard glass fiber with $2a = 62.5 \mu\text{m}$, $\Delta = 0.00962$, we obtain $\Lambda = 1.42 \text{ mm}$. By adopting a coupling length of 1 km (which should be a strict minimum for classical GOF's under normal utilization [11]), this yields a minimum of 706 515 modal interactions required to impact the dispersion. Let us now consider a parabolic-index POF with $2a = 500 \mu\text{m}$ and $\Delta = 0.0126$. The strongest perturbation wavelength is calculated to be $\Lambda = 9.91 \text{ mm}$. This will cause 202 modal interactions over 2 m, which is insufficient to impact the dispersion when compared to the result of glass fiber. For a longer sample of 400 m in length, for example, the number of interactions increases to 40 360, but this number is still 17 times less than that required for the mode-coupling to be efficient. Obviously, the mixing phenomenon is not the reason behind the bandwidth enhancement in GIPOF's. Additional length-dependent power mixing may occur between noncontiguous modes (with smaller Λ), but this is not expected to greatly affect the propagation [9]. Instead of the mode-coupling, we show here that the strong differential mode attenuation which has been given little attention until now is in fact the main cause of the improvement in the fiber dispersion. This trend was recently

shown by some measurements that are to be published in [12], but a proper pulse broadening model which would incorporate the DMA has not been given. This is the topic of this paper that will be discussed in the following sections.

B. Refractive Index and Material Dispersion

We assume that the core and cladding materials of the GIPOF follow a three-term Sellmeier function of wavelength [7], i.e.

$$n_q = \left(1 + \sum_{k=1}^3 \frac{A_{q,k} \lambda^2}{\lambda^2 - \lambda_{q,k}^2} \right)^{1/2} \quad \text{with } q = 1, 2 \quad (9)$$

where $A_{q,k}$ and $\lambda_{q,k}$ are, respectively, the oscillator strength and the oscillator wavelength. The parameters $A_{q,k}$ and $\lambda_{q,k}$ are often gathered under the term of Sellmeier constants. For the ben-doped PMMA GIPOF, these constants are given in [7]. Once the refractive index is known, the material dispersion and the corresponding dispersion slope can be obtained, respectively, from the definitions

$$D = -\lambda n_q'' / c \quad (10)$$

$$S = -(n_q'' + \lambda n_q''') / c. \quad (11)$$

The top part of Fig. 1 reports the refractive index of the cladding and that of the central core region, whilst the bottom part plots the material dispersion as a function of wavelength. In the 650-nm transmission window the previous parameters can be derived as $n_1 = 1.509$, $n_2 = 1.490$, $\Delta = 0.0126$, $N_1 = 1.535$, and $\epsilon = 0.361$. These values allow to theoretically determine the numerical aperture (NA) of the fiber as $NA = (n_1^2 - n_2^2)^{1/2} \simeq 0.24$. On the other hand, the material dispersion at the 650-nm wavelength and the corresponding dispersion slope are calculated approximately to be -403 ps/(nm · km) and 2 ps/(nm² · km), respectively.

C. Simplified Dispersion Model

To allow for clear demonstration, we found it convenient to first present the dispersion analysis within the simplified theory which assumes a uniform excitation and neglects both the effects of distributed loss and mode-coupling. Although these assumptions are invalid in the general case, this analysis should allow for a better understanding of the improved bandwidth model.

Within the weak guidance rule, formula (4) can be approximated by a Taylor series in powers of $\Delta x^{2\alpha/(\alpha+2)}$. The result of a fifth-order expansion is given by

$$\begin{aligned} \tau(x) = & \frac{N_1}{c} \left[1 + \Delta c_1 x^{2\alpha/(\alpha+2)} + \Delta^2 c_2 x^{4\alpha/(\alpha+2)} \right. \\ & + \frac{3}{2} \Delta^3 c_3 x^{6\alpha/(\alpha+2)} \\ & \left. + \frac{5}{2} \Delta^4 c_4 x^{8\alpha/(\alpha+2)} + \frac{35}{8} \Delta^5 c_5 x^{10\alpha/(\alpha+2)} \right] + \dots \end{aligned} \quad (12)$$

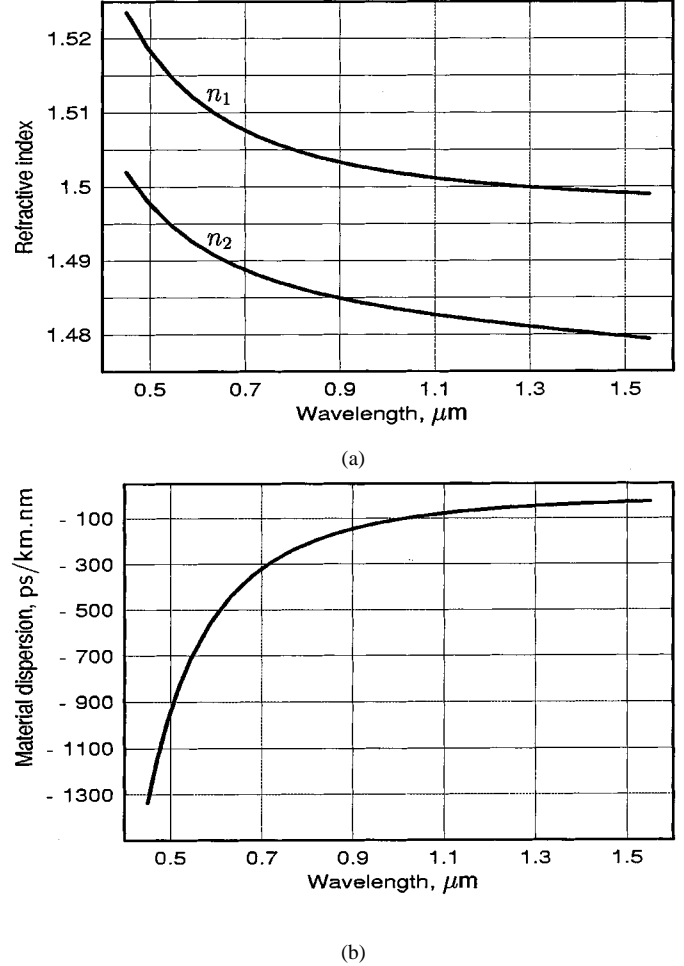


Fig. 1. Refractive index and material dispersion for the ben-doped PMMA GIPOF as a function of wavelength. These results are based on the Sellmeier parameters of [7]: (a) Refractive index of the cladding material and that of the central core region and (b) dispersion of the central core region.

where

$$C_j = \frac{(2j-1)\alpha - 2 - j\epsilon}{j(\alpha+2)} \quad \text{with } j = 1, \dots, 5. \quad (13)$$

Using the above modal delay expression together with the calculation process of [6] (based on evaluating the first three moments of the full impulse response), produces the following expression for the pulse broadening due to chromatic dispersion

$$\begin{aligned} \sigma_{\text{chromatic}} = & \frac{z\sigma_\lambda}{c\lambda_0} \left[(-\lambda_0 n_1'')^2 - 2\lambda_0^2 n_1'' N_1 \Delta c_1 \frac{2\alpha}{2\alpha+2} \right. \\ & + N_1^2 \Delta^2 c_1^2 \frac{(2\alpha)^2}{(\alpha+2)(3\alpha+2)} \\ & + 4N_1^2 \Delta^3 c_1 c_2 \frac{(2\alpha)^2}{(\alpha+2)(4\alpha+2)} \\ & + N_1^2 \Delta^4 (4c_2^2 + 9c_1 c_3) \frac{(2\alpha)^2}{(\alpha+2)(5\alpha+2)} \\ & \left. + N_1^2 \Delta^5 (18c_2 c_3 + 20c_1 c_4) \frac{(2\alpha)^2}{(\alpha+2)(6\alpha+2)} \right]^{1/2}. \end{aligned} \quad (14)$$

In the same way, the intermodal pulse broadening is calculated to be

$$\begin{aligned} \sigma_{\text{modal}} &= \frac{zN_1\Delta}{2c} \frac{\alpha}{\alpha+1} \left(\frac{\alpha+2}{3\alpha+2} \right)^{1/2} \left[c_1^2 + 4\Delta c_1 c_2 \frac{\alpha+1}{2\alpha+1} \right. \\ &\quad + 4\Delta^2 c_2 \frac{(2\alpha+2)^2}{(5\alpha+2)(3\alpha+2)} \\ &\quad + 9\Delta^2 c_1 c_3 \frac{(2\alpha+2)(3\alpha+2)}{(4\alpha+2)(5\alpha+2)} \\ &\quad + 18\Delta^3 c_2 c_3 \frac{(2\alpha+2)^2}{(6\alpha+2)(4\alpha+2)} \\ &\quad \left. + 20\Delta^3 c_1 c_4 \frac{(2\alpha+2)(3\alpha+2)}{(6\alpha+2)(5\alpha+2)} \right]^{1/2}. \end{aligned} \quad (15)$$

The minimum of the modal pulse broadening can be obtained from (15) by solving $(\partial\sigma_{\text{modal}}/\partial\alpha)_{\alpha=\alpha_{\text{opt}}} = 0$. For this, we will retain only the first two terms in (15) as the most relevant. With this approximation it can be shown that the minimum occurs for [6]

$$\alpha_{\text{opt}} = 2 + \epsilon - \Delta \frac{(4+\epsilon)(3+\epsilon)}{5+2\epsilon}. \quad (16)$$

The total rms width of the impulse response, σ_{total} , and the resultant 3-dBo bandwidth can be determined from (14) and (15) as

$$\sigma_{\text{total}} = (\sigma_{\text{chromatic}}^2 + \sigma_{\text{modal}}^2)^{1/2} \quad (17)$$

$$BW = \frac{0.1874}{\sigma_{\text{total}}} \quad (18)$$

The above relations show that the rms width increases in direct proportion to the transmission distance, whilst the bandwidth reduces inversely, i.e., the product of the bandwidth times the length is constant for a given type of fiber. This is the reason why pulse broadening in MMF's has traditionally been described in terms of a constant bandwidth-distance product. But, it should be mentioned in passing that the inclusion of the nonlinear parameters (nonuniform excitation, distributed loss, eventual mode-coupling) will cause the bandwidth-distance product to depend on length to a certain degree. So this concept will no longer be meaningful in characterizing the fiber dispersion behavior. Instead, the determination of the bandwidth-versus-length characteristic will be relevant for link designers.

It is of interest to compare formula (14) and (15) with equivalent expressions derived by Olshansky and Keck. Firstly, we note that the third term in (46) of [6] involves a multiplying factor $2\alpha/(3\alpha+2)$. Instead, the present intermodulation dispersion formula (14) involves $4\alpha^2/[(\alpha+2)(3\alpha+2)]$, which is quite in agreement with the correction already reported by Soudagar and Wali [13]. Secondly, it is noteworthy that our calculation incorporates more terms in the expressions of the chromatic and intermodal pulse broadenings compared to those displayed in [6]. This follows from the fact that we used a fifth order expansion of the modal delay instead of a second order expansion as

did Olshansky and Keck [6]. For a system operated within the standard low-loss transmission windows, the contribution of the extra terms may not be significant as long as the weak guidance rule remains valid. Their effect will become important if the numerical aperture (NA) of the fiber in consideration is fairly high and if a nearly zero material dispersion wavelength is used. Therefore, dispersion formula [14] and [15] can be regarded as refinements to Olshansky and Keck's expressions.

D. Full Dispersion Analysis

We consider a multimode fiber characterized by the α -class refractive index profile defined in (1) as linear in its input-output relationship [14]. In this case, we have recently shown that within some conditions that are expected to be satisfied in practice, the complex transfer function of such MMF's can be modeled by a product of two filter functions as follows [15]

$$H_{\text{MMF}}(z, \omega) = H_{\text{chromatic}}(z, \omega) H_{\text{modal}}(z, \omega) \quad (19)$$

where $H_{\text{chromatic}}(z, \omega)$ and $H_{\text{modal}}(z, \omega)$ represent chromatic dispersion and modal dispersion, respectively. The parameters appearing in argument of both functions are the baseband angular frequency ω , and the transmission length z .

Equation (19) expresses the latent idea that chromatic and modal dispersions are independent effects and can be evaluated separately. Under the assumption that the power spectral density of the driving source has a Gaussian lineshape with rms linewidth σ_λ , the chromatic transfer function can be calculated exactly, yielding [15], [16]

$$H_{\text{chromatic}}(z, \omega) = \frac{1}{(1 + i\omega/\omega_2)^{1/2}} \exp \left[-\frac{(\omega/\omega_1)^2}{2(1 + i\omega/\omega_2)} \right] \quad (20)$$

in which ω_1 and ω_2 have been introduced as abbreviations for

$$\omega_1 = -(\sigma_\lambda D_0 z)^{-1} \quad (21)$$

$$\omega_2 = [\sigma_\lambda^2 (S_0 + 2D_0/\lambda) z]^{-1} \quad (22)$$

where D_0 is the modal velocity dispersion averaged over all guided modes and S_0 is the averaged dispersion slope. It is important to realize that for a system operated around a zero material dispersion wavelength, the chromatic effect is not necessarily negligible because of the presence of the dispersion slope. Therefore, this term cannot be systematically ignored even in the zero dispersion region. The fact that averaged values are used for the dispersion and dispersion slope may cause the chromatic transfer function as defined in (20) to slightly depend on all parameters that determine the propagation, i.e., launch conditions, distributed loss and mode-coupling. We have to mention, however, that, after computation at the 650-nm wavelength, we have not recorded any significant difference between these averaged values compared to those calculated previously by considering only the material contribution, i.e., $D_0 \simeq -403$ ps/(nm · km) and $S_0 \simeq 2$ ps/(nm² · km).

The modal transfer function is given by

$$H_{\text{modal}}(z, \omega) = \frac{\int_{x_0}^1 2xR(x, z, \omega) dx}{\int_{x_0}^1 2xR(x, z, 0) dx} \quad (23)$$

where $x_0 = 1/M$, $x = m/M$ and $R(x, z, \omega)$ is the modal power in Fourier domain. The numerator in the right hand side of (23) is a normalization factor representing the total power at position z . As a general rule, $R(x, z, \omega)$ is a solution of a partial differential equation (referred to as power flow equation or diffusion equation) which incorporates not only the modal delay but also the distributed loss and mode-coupling effects. The power flow equation has no analytical solutions and can be solved only numerically. Such an analysis was previously carried out in [15] concerning glass fibers and could readily be extended to GIPOF's. As we explained in Section II-A, the contribution of the mode-coupling phenomenon should be negligible over the lengths of GIPOF samples usually considered. In this case the modal power can simply be calculated as

$$R(x, z, \omega) = C_{\text{rmeff}}(x) \exp[-\gamma(x)z] \exp[-i\omega\tau(x)z] \quad (24)$$

where $C_{\text{rmeff}}(x)$ is the mode excitation coefficient (or coupling/launching efficiency), and $\gamma(x)$ is the mode-dependent attenuation. The fact that it is the difference in the modal parameters that causes the intermodal dispersion can readily be verified from the expressions (23) and (24). Indeed, it is clear that the shape of the frequency response will not be affected by multiplying (24) by any overall constant factor. Thus, $\gamma(x)$ could be replaced by $\gamma(x) - \gamma(x_0)$ which represents the differential mode attenuation. In the same way, $\tau(x)$ could be replaced by $\tau(x) - \tau(x_0)$ which represents the differential mode delay (DMD).

To enable further frequency response simulations to be done incorporating all the parameters involved, the mode excitation coefficients as well as the differential mode attenuation must be specified. Let us discuss these aspects in two separate Sections.

1) Excitation Coefficients: The presence of the excitation coefficient in (24) permits to use the present model under any launching condition. $C_{\text{rmeff}}(x)$ can be evaluated as the overlap integral of the electrical field of each fiber mode with the electrical field of the incident light. If we consider that the fiber launching is uniform as did Olshansky and Keck, the initial power distribution is by assumption the same for each mode and $C_{\text{rmeff}}(x)$ can be formally set to unity. This approximation is realistic if a light emitting diode is being used as a launching source. But most of experiments so far carried out on the PMMA GIPOF's employ visible light beams from semiconductor lasers. Therefore, it is closest to reality to adopt the assumption of a Gaussian-type shape for the input beam spot [17].

We will additionally assume that the fiber is excited centrally with a laser beam that forms a circularly symmetric spot on the input surface. It is equally considered that the fiber axis is well aligned with the beam axis, and that its end surface is well positioned in the focal plane. The field of such a beam can be

expressed in cartesian coordinate (with the core center taken as the origin of axes) as

$$E_{in}(x, y) = \frac{\sqrt{2}}{\sqrt{\pi}w} \exp\left(-\frac{x^2}{w^2}\right) \exp\left(-\frac{y^2}{w^2}\right) \quad (25)$$

where w stands for the beam spot radius.

We also adopt the simplified approximation that the launching field given above excites solely the Hermite–Gauss fields of the fiber given by [18]

$$\psi_{\mu\nu}(x, y) = \frac{1}{w_0 \sqrt{\pi 2^{\mu+\nu} \mu! \nu!}} H_{\mu}\left(\frac{\sqrt{2}x}{w_0}\right) H_{\nu}\left(\frac{\sqrt{2}y}{w_0}\right) \exp\left(-\frac{x^2 + y^2}{w_0^2}\right) \quad (26)$$

where H_{μ} is the Hermite polynomial of degree μ and w_0 is referred to as the beam radius of the fundamental modes given by

$$w_0 = \frac{1}{(2\Delta)^{1/4}} \left(\frac{\lambda a}{\pi n_1}\right)^{1/2}. \quad (27)$$

The overlap integral of (25) and (26) is calculated from the following definition where the integration is taken over the input plane

$$a_{\mu\nu} = \int_{(A)} E_{in}(x, y) \psi_{\mu\nu}(x, y) dx dy. \quad (28)$$

This integral can be solved exactly, yielding [19]

$$a_{\mu\nu} = \begin{cases} 0 & \text{for } \mu \text{ or } \nu \text{ odd} \\ \frac{\sqrt{2}}{\pi w_0 w \sqrt{2^{\mu+\nu} \mu! \nu!}} I_{\mu} I_{\nu} & \text{for } \mu \text{ and } \nu \text{ even.} \end{cases} \quad (29)$$

in which

$$I_{\mu} = w_0 (-1)^{\mu/2} 2^{\mu-1} \cdot \frac{\Gamma(1/2) \Gamma[(\mu+1)/2]}{\sqrt{\pi z_0/2}} F(-\mu/2, 1/2, 1/2, 1/z_0) \quad (30)$$

$$z_0 = \frac{1}{2} + \frac{w_0^2}{2w^2} \quad (31)$$

where $\Gamma(x)$ is the gamma function and $F(x_1, x_2, x_3, x_4)$ is the hypergeometrical function.

The mean power excitation coefficient of modes in group m , that we denote by C_m , can be derived from (29) as

$$C_m = \frac{1}{2m} \sum_{\mu=0}^{m-1} |a_{\mu, m-\mu-1}|^2. \quad (32)$$

The excitation coefficient as a function of the normalized group number x can be calculated as follows. During the numerical evaluation of (23), using for example Simpson rule, the variable x is handled as discrete values x_i . From each of these discrete values x_i , the corresponding mode group number m is derived as the integer nearest to the product Mx_i and the

x -dependent excitation coefficient is simply computed by identifying $C_{rmeff}(x_i)$ to C_m .

2) *Differential Mode Attenuation*: The other parameter required in the computation of the modal transfer function is the differential mode attenuation. The modal attenuation originates from conventional loss mechanisms that are present in a usual fiber, that is, absorption [20], Rayleigh scattering [20] and loss on reflection at the core-cladding interface [21]. These different loss mechanisms act on each mode in a different manner, which causes the attenuation coefficient to vary from mode to mode. For example the fiber boundary has a strong effect on modes near cutoff but little on the fundamental ones. Because of the multiple origins of the DMA, the modeling of this phenomenon is not an easy task. Even though we may succeed through simplifying assumptions, the resulting model will inevitably introduce a number of parameters for which it may be difficult to find correct numerical values. We believe that as it is a common practice to systematically measure a fiber attenuation in the usual transmission windows, it should be the same for the DMA. Such measured data could readily be incorporated in the dispersion model by fitting an appropriate function. For this, we suggest to use the following functional expression for the distributed loss

$$\gamma(x) = \gamma_0 + \gamma_0 I_\rho[\eta(x - x_0)^{2\alpha/(\alpha+2)}] \quad (33)$$

where γ_0 is the attenuation of low-order modes, I_ρ is the ρ th-order modified Bessel function of the first kind, and η is a weighting constant.

The question now is to put proper numerical values on the parameters appearing in formula (33), for the computation to be possible. Unfortunately, no measured DMA data for POF's exist in the literature yet. However, various measurements on glass optical fibers show that, more than anything, the DMA in decibels as a function of the principal mode group number depends on the wavelength and on the numerical aperture (NA) [20], [22]. In other words, the fiber materials seem to have no significant effect on the DMA shape as long as the refractive index conforms to a circular-symmetric profile law in accordance with the definition (1). Therefore, we will adopt the profile of [22, Fig. 7(c)], but we will vertically shift the curve to accommodate the estimated minimum attenuation of 124 dB/km of POF's [23]. Although a modification of the data is proposed for POF's, this approximation that the DMA profile is the same as that of GOF's may seem rough at first glance, in particular if account is taken of a possible influence of the size of the core. Because, the numerical results obtained here are quite in line with previous transmission experiments, as we explain further, we believe that this assumption should present a large degree of validity. The results are reported in Fig. 2. The fitting of measurements of [22] to the empirical expression (33) leads to $g_0 \simeq 2.8 \cdot 10^{12} \text{ km}^{-1}$, $\rho \simeq 11$ and $\eta \simeq 12.2$. It is worth noticing from these values that the strength of the DMA in POF's follows mainly from the fact that the minimum attenuation is extremely large. For comparison, the minimum attenuation of single cladded fluoride glass fibers in the 1300 nm transmission window is less than 1 dB/km, that is, $g_0 < 1.26 \text{ km}^{-1}$. Future experiments on POF samples could be done for a better understanding of the DMA behavior.

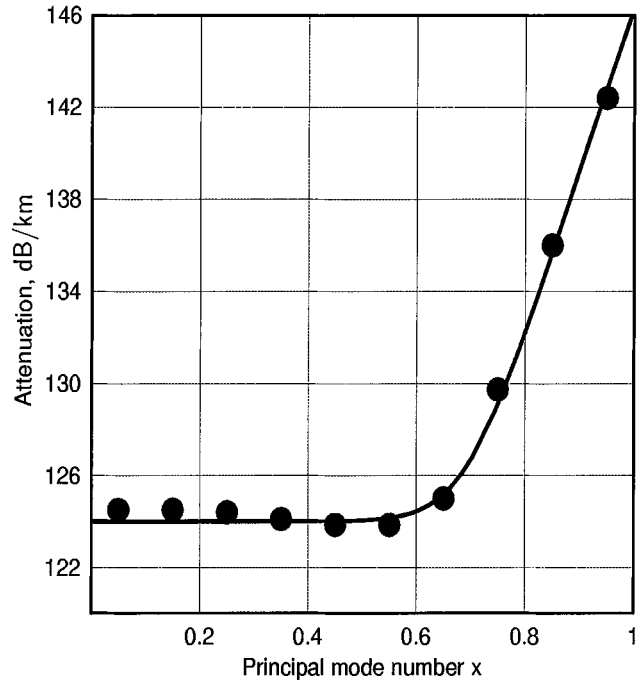


Fig. 2. Mode-dependent attenuation (MDA) as a function of the normalized mode order x : The bullets represent the measurements reported in [22, Fig. 7(c)], whilst the solid curve is the fitted MDA formula (33) with $\rho = 11$ and $\eta = 12.2$. Note that the curve is properly shifted in order to take the minimum attenuation of 124 dB/km into account.

III. SIMULATION RESULTS

We have carried out computer simulations for the graded-index type POF having a PMMA uniform cladding and a gradually varying concentration of benzyl benzoate dopant in the core [7]. It is assumed that the exciting light source emits a visible light near 650 nm and has an rms linewidth of 0.5 nm. These are the characteristics of the MQW laser diode specially developed by NEC Co. for high-performance POF systems, and that we used in previous transmission experiments [3], [4].

Fig. 3 reports the chromatic, intermodal and total bandwidth of a 100 m-long PMMA GIPOF as a function of the core refractive index exponent for the 650-nm wavelength. These plots are based on the analysis of Section II-C which assumes a uniform excitation and neglects both the distributed attenuation and mode-coupling. The chromatic bandwidth is seen to show little dependence on α , which means that the material dispersion is the dominant contribution in the transmission window considered. On the other hand, the modal bandwidth shows a highly peaked resonance with α . This is the well-known characteristic feature of the grading. With the present choice of parameter-values, the maximum turns out to be located around an α -factor of 2.33, which quite corresponds to the value calculated from expression (16). Another result that can be noted from Fig. 2 is the presence of crossover points at $\alpha_1 \simeq 2.27$ and $\alpha_2 \simeq 2.39$ between the chromatic and modal characteristics. This shows that the total bandwidth may mainly be limited either by the modal dispersion or the chromatic dispersion depending on the value of the index exponent. As shown by the solid curve in Fig. 2, the chromatic dispersion will essentially

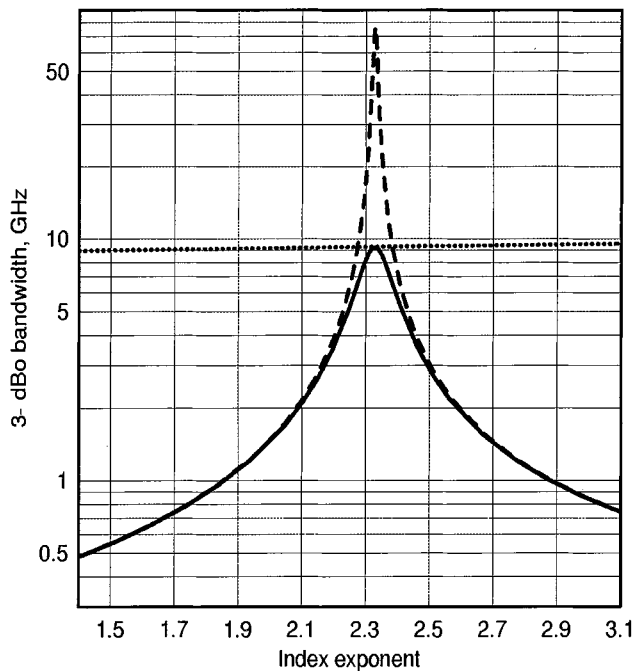


Fig. 3. 3-dBo baseband bandwidth of a 100-m-long fiber as a function of refractive index exponent for a 650-nm wavelength. All three curves are based on the results of analysis presented in Section II-C: (—) Total bandwidth, (---) Modal bandwidth, (·····) Chromatic bandwidth.

limit the total bandwidth for $\alpha_1 < \alpha < \alpha_2$, whilst for $\alpha < \alpha_1$ or $\alpha > \alpha_2$ the modal dispersion will cause the main limitation. But these comments are valid only if the approximations related to this model are likely to be satisfied. We will show further that the modal response of the GIPOF greatly enhances due to the strong differential mode attenuation.

Before discussing the full dispersion analysis through illustrations, it is of interest to firstly verify its consistency with Olshansky and Keck's theory when the same approximations are imposed. For this, a series of frequency response simulations has been done under the assumption of uniform excitation, constant mode attenuation and absence of mode-coupling. Some of these results are displayed in Fig. 4 where plots of the fiber frequency response for a sample length of 100 m and a varying index exponent of 2.1, 2.3, and 2.4 are given. The 3-dB baseband bandwidths corresponding to the three values of α are found approximately to be 2.0, 8.3, and 5.6 GHz, respectively. These values exactly match with those obtained from formula (18). We have also separately verified through various numerical simulations, not reported here, that the chromatic and modal bandwidths calculated from expressions (20) and (23) coincide well with the values calculated from formula (14) and (15), respectively. Let us mention *a posteriori* that the bandwidth is defined here as the half-power frequency of the modulus of the transfer function over the distance considered.

The modal frequency response simulations are displayed in Fig. 5, where the effects of the launching condition and that of the differential mode attenuation are shown. For comparison a dotted curve is reported in the same figure representing the frequency response due to chromatic dispersion. These results indicate that both the Gaussian beam excitation (with overfilled core diameter) and the presence of DMA are favorable for im-

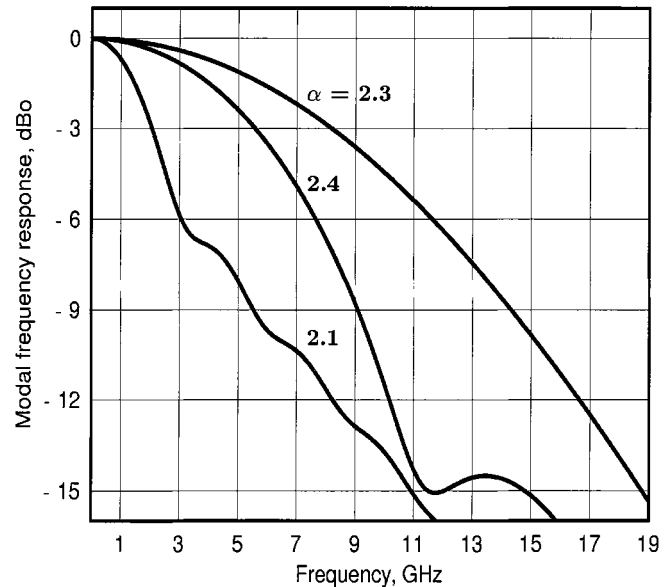


Fig. 4. Frequency responses of a 100-m-long PMMA GIPOF for a wavelength of 650 nm and varying index exponent $\alpha = 2.1, 2.3, 2.4$. These plots result from formula (19) within the assumption of a uniform excitation in the absence of distributed loss and mode-coupling.

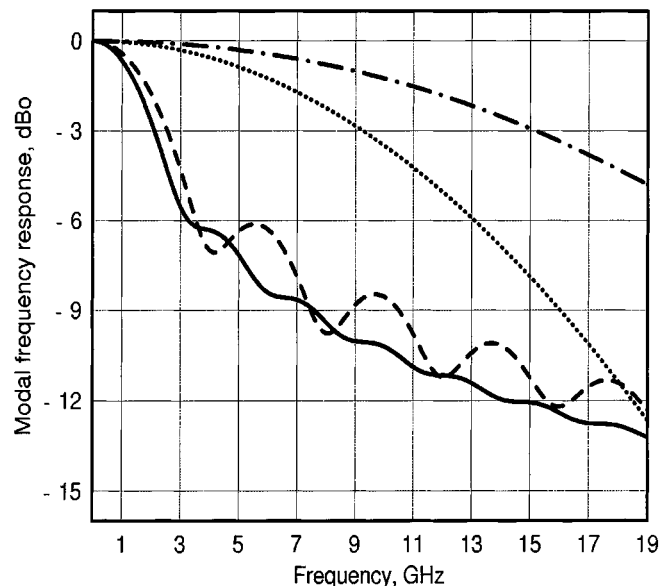


Fig. 5. Modal frequency responses of a 100-m-long PMMA GIPOF for an index exponent of 2.1 and a wavelength of 650 nm: (—) Uniform excitation without DMA, (---) Gaussian beam excitation ($w = 250\mu\text{m}$) without DMA, (- · -) Uniform excitation with DMA; The dotted curve represents the chromatic frequency response given for comparison.

proving the modal response of the GIPOF. It can be observed, in particular, that the bandwidth enhancement caused by the DMA is dramatically large. The modal response with DMA is even seen to become superior to the response due to chromatic dispersion. Obviously, this result shows that the DMA is a determining factor for accurate assessment of the baseband bandwidth in POF's, and consequently it cannot be excluded from the model as it has been the case for glass fibers.

Fig. 6 plots the total fiber bandwidth as a function of transmission length, showing a comparison between Olshansky and Keck's theory and the improved model including the effect of

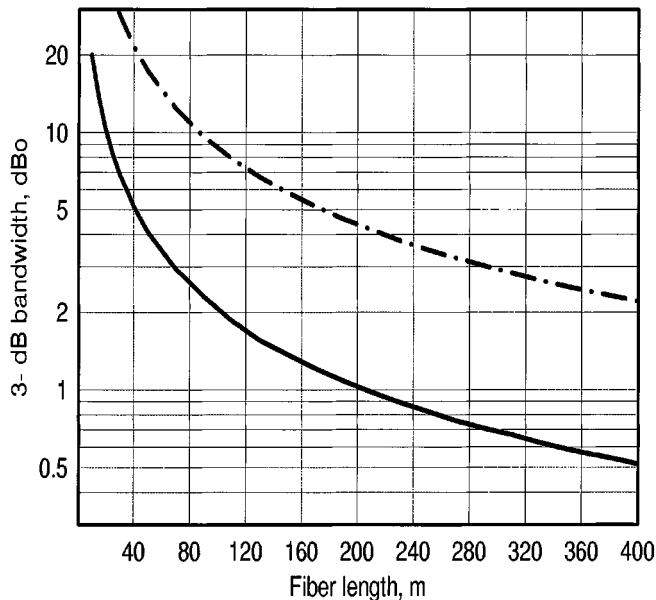


Fig. 6. Total 3-dB bandwidth of the PMMA GIPOF as a function of transmission length for an index exponent of 2.1 and a wavelength of 650 nm: (—) Result of formula (18), (- · -) Result of formula (23) including DMA.

DMA. It is clear again that the DMA enhances the total bandwidth to a considerable extent. Indeed, it can be seen from the figure that at least a fourfold bandwidth enhancement may be gained. For example, the 3-dB bandwidth corresponding to a 200-m-long sample is found from the simplified dispersion model to be 1.0 GHz but it increases to 4.4 GHz in the presence of DMA. This result is more consistent with the error-free transmission experiment at 2.5 Gb/s that we achieved in [3], [4]. Most important, the dash-dot curve of Fig. 6 indicates that the PMMA GIPOF has greater potential than suggested by previous experiments. It appears that the data rate can be increased up to 8.7 and 4.4 Gb/s through the 100- and 200-m-long samples, respectively, if the laser source is capable of such modulation speeds. An error-free transmission at a bit rate of 2.5 Gb/s via a 300-m GIPOF can even be realized. These predicted figures should be verified in future experiments. Consequently, it has become a reality that the PMMA GIPOF can span longer distances than those foreseen so far. As an example, one could envisage the coverage of medium-size building backbones with this type of GIPOF provided that a sufficient power budget can be made available.

IV. DISCUSSION

As mentioned before, the fact that the GIPOF bandwidth increases with a strong differential mode attenuation is unsurprising. During the propagation of light through the fiber, high-order modes that have the fastest attenuation gradually lose their energy and only a small fraction of the number of guided modes supported by the waveguide have significant power to be detected. In other words, the bandwidth enhancement follows from the filtering effect of the DMA. This in fact reflects the classical trade-off relation between dispersion and loss in multi-mode fibers in general.

It is also of interest to mention that because the bandwidth of the GIPOF is essentially limited by material dispersion (as a consequence of the DMA effect), its operation under a restricted mode excitation using the techniques described in [24] to support increased transmission rates in GOF's should not result in a significant bandwidth improvement. Nevertheless, a selective mode launching scheme could be implemented in the view of benefiting from the minimum loss advantage. In that case, indeed, low-order modes are involved that propagate near fiber axis with the slowest attenuation, which should cause a dramatic reduction of the inline power penalty. A limited mode launch of the GIPOF in the center of the core may reduce the mean attenuation of 164 dB/km [3], [4] to the minimum of 124 dB/km [23] or less. In other words, the 32.8-dB power loss over the 200-m-long sample may drop to 24.8 dB or less. In this way one could release at least 8 dB in the power budget, thereby allowing for a less sensitive and certainly less expensive receiver to be employed.

In summary, since the DMA in GIPOF's affects both dispersion and loss to a considerable degree, it becomes a determining factor in the choice of system parameters. Accordingly, a good knowledge of the DMA will be of prime importance for link designers and users. Also, always owing to the large effect of this parameter, its clear understanding can no longer be bypassed if appropriate network standards are to be developed. Although a distributed loss curve that would directly be measured using a GIPOF sample is not expected to depart as much from the shape of Fig. 2, this experiment needs to be done in future.

V. CONCLUSION

We have described the dispersion behavior of laser-based graded-index polymer optical fiber systems. This model incorporates all parameters involved in the determination of the baseband bandwidth, in particular, the differential mode attenuation that was ignored in the standard theory. The mathematical development is based on analytically evaluating the frequency response of the fiber instead of the direct calculation of the pulse broadening from the moments of the impulse response. It can be used at any wavelength under any input condition including the fiber excitation by a Gaussian-shape beam spot which is closest to most practical applications.

We have shown that the 3-dB bandwidth is enhanced in GIPOF's mainly due to the strong DMA. The numerical results are quite in line with the transmission performances obtained previously. Since this simulation tool can be used to establish more likely performance limits, it should be useful to the design of more reliable GIPOF systems. We believe that this analysis is an important milestone for the development of gigabit links in graded-index polymer optical fibers.

ACKNOWLEDGMENT

The author would like to thank Prof. G. D. Khoe, Dr. H. de Waardt, and Ir. H. P. A. van den Boom for continuous and helpful discussions. He equally acknowledges useful discussions with Dr. T. Ishigure from Keio University, Japan, about the parameters of the PMMA material.

REFERENCES

- [1] T. Ishigure, E. Nihei, S. Yamazaki, K. Kobayashi, and Y. Koike, "2.5 Gbit/s 100 m data transmission using graded-index polymer optical fiber and high-speed laser diode at 650 nm wavelength," *Electron. Lett.*, vol. 31, pp. 467–468, 1995.
- [2] Y. Koike, T. Ishigure, and E. Nihei, "High-bandwidth graded-index polymer optical fiber (Invited Paper)," *J. Lightwave Technol.*, vol. 13, pp. 1475–1489, 1995.
- [3] W. Li, G. D. Khoe, H. P. A. v.d. Boom, G. Yabre, H. de Waardt, Y. Koike, M. Naritomi, N. Yoshihara, and S. Yamazaki, "Record 2.5 Gbit/s transmission via polymer optical fiber at 645 nm visible light," in *Proc. 7th Int. Conf. Plastic Optical Fibers Appl. (POF'98)*, Berlin, Germany, Oct. 1998, (Postdeadline paper).
- [4] W. Li, G. Khoe, H.v.d. Boom, G. Yabre, H. de Waardt, Y. Koike, S. Yamazaki, K. Nakamura, and Y. Kawaharada, "2.5 Gbit/s transmission experiment over 200 m PMMA graded index polymer optical fiber using 645 nm narrow spectrum laser and a silicon APD," *Microwave Optic. Technol. Lett.*, vol. 20, pp. 163–166, 1999.
- [5] G. D. Khoe, Y. Koike, T. Ishigure, P. K.v. Bennekomp, H. P. A.v.d. Boom, W. Li, and G. Yabre, "Status of GIPOF systems and related technologies (Invited paper)," in *Proc. 25th Eur. Conf. Optical Commun. (ECOC'99)*, Nice, France, Sept. 1999.
- [6] R. Olshansky and D. B. Keck, "Pulse broadening in graded-index optical fibers," *Appl. Opt.*, vol. 15, pp. 483–491, 1976.
- [7] T. Ishigure, E. Nihei, and Y. Koike, "Optimum refractive-index profile of the graded-index polymer optical fiber, toward gigabit data links," *Appl. Opt.*, vol. 35, pp. 2048–2053, 1996.
- [8] A. F. Garito, J. Wang, and R. Gao, "Effects of random perturbations in plastic optical fibers," *Science*, vol. 281, pp. 962–967, 1998.
- [9] R. Olshansky, "Mode coupling effects in graded-index optical fibers," *Appl. Opt.*, vol. 14, pp. 935–945, 1975.
- [10] S. D. Personick, "Time dispersion in dielectric waveguides," *Bell Syst. Tech. J.*, vol. 50, pp. 843–859, 1971.
- [11] K.-I. Kitayama, S. Seikai, and N. Uchida, "Impulse response prediction based on experimental mode coupling coefficient in a 10-km long graded-index fiber," *IEEE J. Quantum Electron.*, vol. 16, pp. 356–362, 1980.
- [12] T. Ishigure, M. Kano, and Y. Koike, "Which is serious factor to the bandwidth of GIPOF: Mode dependent attenuation or mode coupling?," in *Proc. 25th Eur. Conf. Optical Commun. (ECOC'99)*, Nice, France, Sept. 1999.
- [13] M. K. Soudagar and A. A. Wali, "Pulse broadening in graded-index optical fibers: Errata," *Appl. Opt.*, vol. 32, p. 6678, 1993.
- [14] S. D. Personick, "Baseband linearity and equalization in fiber optic digital communication systems," *Bell Syst. Tech. J.*, vol. 52, pp. 1175–1195, 1973.
- [15] G. Yabre, "Comprehensive theory of dispersion in graded-index optical fibers," *J. Lightwave Technol.*, Feb. 2000, to be published.
- [16] E.-G. Neumann, *Single-Mode Fibers*. Berlin, Heidelberg, Germany: Springer-Verlag, 1988, pp. 246–247.
- [17] T. P. Lee, C. A. Burrus, D. Marcuse, A. G. Dentai, and R. J. Nelson, "Measurement of beam parameters of index-guided and gain-guided single-frequency InGaAsP injection lasers," *Electron. Lett.*, vol. 18, pp. 902–904, 1982.
- [18] D. Marcuse, *Light Transmission Optics*. New York: Van Nostrand Reinhold, 1972.
- [19] J. Saijonmaa and S. J. Halme, "Reduction of modal noise by using reduced spot excitation," *Appl. Opt.*, vol. 20, pp. 4302–4306, 1981.
- [20] R. Olshansky and D. A. Nolan, "Mode-dependent attenuation of optical fibers: Excess loss," *Appl. Opt.*, vol. 15, pp. 1045–1047, 1976.
- [21] D. Gloge, "Weakly guiding fibers," *Appl. Opt.*, vol. 10, pp. 2252–2258, 1971.
- [22] A. R. Mickelson and M. Eriksrud, "Mode-dependent attenuation in optical fibers," *J. Opt. Soc. Amer.*, vol. 73, pp. 1283–1291, 1983.
- [23] Club des Fibers Optiques Plastiques (CFOP), *Plastic Optical Fibers—Practical Applications*. New York: Wiley, 1997.
- [24] Z. Haas and M. A. Santoro, "A mode-filtering scheme for improvement of the bandwidth-distance product in multimode fiber systems," *J. Lightwave Technol.*, vol. 11, pp. 1125–1131, 1993.



Gnitabouré Yabre (M'97) was born in Boutaya-P/Zabré, Burkina Faso, in 1962. He received the D.E.A. degree in electronics and the Doctorate degree in optronics, both from the University of Brest, France, in 1989 and 1993, respectively.

From 1989 to 1995, he worked in the RESO laboratory at the "Ecole Nationale d'Ingénieurs de Brest," France. He is now with COBRA, Interuniversity Research Institute, Eindhoven University of Technology, The Netherlands. During his previous post, his research activities were focused on semiconductor laser nonlinearities, linearization alternatives, injection-locking, subcarrier-multiplexing techniques, fiber-to-wireless communication systems, broad-band optical communication systems, and networks. He is currently working on communication multimode optical fibers and related systems.

Dr. Yabre has served as a reviewer for the JOURNAL OF LIGHTWAVE TECHNOLOGY, IEEE TRANSACTIONS ON MICROWAVE THEORY AND TECHNIQUES, and *Optics Communications*.